7. W. H. Bakun and T. V. McEvilly, *ibid.* **205**, 1375 (1979); *J. Geophys. Res.* **89**, 3051 (1984).
8. P. E. Malin, S. N. Blakeslee, M. G. Alvarez, A. J. Martin, *Science* **244**, 557 (1989), T. V. McEvily *et al.*, *U.S. Geol. Surv. Open-File Rep. 89-453* (1989), p. 333.
9. K. Aki, *J. Geophys. Res.* **84**, 6140 (1979); W. D. Mooney and J. H. Luetgert, *Bull. Seismol. Soc. Am.* **72**, 901 (1982); A. P. Papageorgiou and K. Aki, *ibid.* **73**, 953 (1983).
10. K. Aki and W. H. K. Lee, *J. Geophys. Res.* **81**, 4381 (1976); C. H. Thurber, *ibid.* **88**, 8226 (1976).
11. R. Feng and T. V. McEvilly, *Bull. Seismol. Soc. Am.* **73**, 1701 (1983); J. N. Louie, R. W. Clayton, R. J. LeBras, *Geophysics* **53**, 176 (1988).
12. C. Y. Wang, *J. Geophys. Res.* **89**, 5858 (1984).
13. J. H. Dietrich, *ibid.* **84**, 2161 (1979); *ibid.*, p. 2169; W. D. Stuart, R. Archuleta, A. G. Lindh, *ibid.* **92**, 592 (1985); T. Cao and K. Aki, *Pure Appl. Geophys.* **122**, 10 (1984/85).
14. K. Aki, *J. Geophys. Res.* **92**, 1349 (1987); P. Okubo and K. Aki, *ibid.*, p. 345.
15. This investigation was supported in part by DOE contract DE-FG03-87ER13807 and by NSF grants EAR-8213145 and EAR-8519938.

19 March 1990; accepted 8 June 1990

Precessional Forcing of Nutricline Dynamics in the Equatorial Atlantic

B. MOLFINO AND A. MCINTYRE

Climate control of nutricline depth in the equatorial Atlantic can be monitored by variations in the abundance of the phytoplankton species *Florisphaera profunda*. A conceptual model, based on in situ evidence, associates high abundances of *F. profunda* with a deep nutricline and low abundances with a shallow nutricline. A 200,000-year record of *F. profunda* relative abundances, obtained from a deep-sea core sited beneath the region of maximum equatorial divergence at 10°W, has 52 percent of its variance centered on the 23,000-year precessional band. Cross-spectral analysis between the signals of *F. profunda* and sea-surface temperature, independently derived from zooplankton species, shows their 23,000-year cycles to be coherent and nearly in phase. Abundance minima of *F. profunda* coincide with times of December perihelion, whereas abundance maxima coincide with June perihelion. These relations indicate that nutricline dynamics in the divergence region of the equatorial Atlantic are controlled by variations in the tropical easterlies, forced by the precessional component of orbital insolation, on time scales greater than 10,000 years.

THE TURBULENT BOUNDARY LAYER (TBL) is the upper layer of the ocean where exchange of heat and mass occurs between the oceanic and atmospheric reservoirs. The physical oceanography of the TBL is a major factor in atmosphere-ocean dynamics on all time scales. On time scales encompassed by the instrumental record, knowledge of the observed and modeled annual and interannual dynamics of the TBL is progressing rapidly (*1*). On paleoceanographic time scales, knowledge of the structure of the TBL is lacking. Paleoindicators that vertically partition the TBL to measure the character of the layers (above and below the thermocline) are needed. In this report, we present a conceptual model of the coccolithophorid (chrysophycean) species *F. profunda*. Our model is based on in situ observation, and it allows us to predict *F. profunda* variations as a function of nutricline dynamics. We applied this model to the oceanic sediments of the equatorial Atlantic in two ways: (i) spatially, using a meridional transect of modern sediment samples that compares *F. profunda*'s response to known variations of nutricline depth; and (ii) temporally, using a 200,000-year record of *F. profunda* response from one core in this transect. This species shows that nutricline dynamics in the equatorial Atlantic respond to the precessional component of insolation forcing.

Okada established the gross biogeography and ecology of *F. profunda*. This marine alga is restricted to the lower euphotic zone at temperatures >10°C (*2*), as documented for tropical and subtropical TBLs of the Pacific and the Atlantic oceans (*2–4*). All other coccolithophorids that are preserved in the fossil record are restricted to the upper euphotic zone. *Florisphaera profunda* produces subrectangular calcite plates (mean of 2.5 μm) that are easily recognized in the electron microscope and are well preserved in oceanic sediments (*2*).

We suggest that *F. profunda* can be used to monitor variations in the depth of the nutricline. Our conceptual model uses a partitioned euphotic zone in which the controlling mechanism is variation in nutrient concentration of the upper euphotic zone (Fig. 1). The random variable is the depth of the nutricline; the response variables are the number of *F. profunda* and the number of other coccolithophorids. A deep nutricline means the upper euphotic zone is nutrient-depleted and hence *F. profunda*'s production is enhanced relative to other coccolithophorids; a shallow nutricline has the opposite effect. We identified 500 individuals per sample and computed the percentage of *F. profunda* in the total sample as our measure of variation. The sample counts are binomially distributed; their statistical error (95% confidence limits based on binomial proportions, $n = 500$) is approximately ±4% for values between 30 and 70% (*5*).

In the equatorial Atlantic, alternating ribbons of high and low primary productivity are aligned along parallels of latitude (*6*). These ribbons are produced by the seasonally varying surface currents of the South

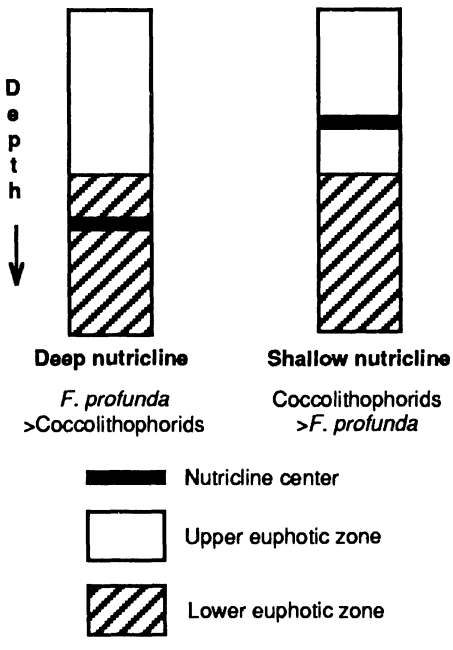

Fig. 1. The conceptual model of *F. profunda* response to variation in nutricline depth is illustrated with two end member scenarios. *Florisphaera profunda* is restricted to the lower part of the euphotic zone, while all other coccolithophorid species inhabit the upper euphotic zone. A deep nutricline enhances the production of *F. profunda* over all other coccolithophorid species (left). A shallow nutricline enhances the production of other coccolithophorid species relative to *F. profunda* (right).

B. Molfino, Lamont-Doherty Geological Observatory of Columbia University, Palisades, NY 10964, and Department of Statistics, Columbia University, New York, NY 10027.
A. McIntyre, Lamont-Doherty Geological Observatory of Columbia University, Palisades, NY 10964, and Department of Geology, Queens College of the City University of New York, Flushing, NY 11357.

Equatorial Current (SEC), the Equatorial Undercurrent (EU), and the North Equatorial Countercurrent (7). Maximum nutricline and thermocline shallowing, due to divergence, is centered on 10°W in the SEC (8). Here the contact between the westward-flowing SEC, aligned on 4°S, and the eastward-flowing EU, aligned on 0°, is delineated by major changes in many physical parameters (7, 9), for example, nutrient and oxygen content.

We have counted *F. profunda* in a north-south transect of 11 surface sediment samples, aligned on 11°30′W (Fig. 2). The rapid change in the percentage of *F. profunda* in the equatorial transect marks the contact between the SEC and the EU, which rises to its shallowest depth at 10°W. This contact is associated with the boundary between high values of phosphate in the euphotic zone to the south and low values of phosphate in the euphotic zone to the north; the depth of the nutricline, defined by a level of PO_4 of 1.0 μmol liter^{-1} (10), varies between 50 and 200 m (9, 11). Although the abundance of many planktonic organisms (for example, foraminifera and other coccolithophorid species) changes across this boundary, the abundance variation of *F. profunda* has the greatest amplitude. Its response records a decrease in coccolith production in the upper euphotic zone by an increase in relative abundance. Thus, in this spatial study, observation and model agree: low percentages of *F. profunda* are associated with a shallow nutricline and, by proxy, a shallow thermocline, and high percentages of *F. profunda* are associated with a deep nutricline and, by proxy, a deep thermocline. No other extant coccolithophorid species that is also preserved in the fossil record has this signature.

In the equatorial Atlantic the region of maximum divergence is in the region of maximum heat flux into the ocean. Vast quantities of heat and gas interchange vertically with the atmosphere and horizontally between the oceans of the Northern and Southern hemispheres. These interchanges are controlled by advection that is modulated by the tropical easterlies, which are forced by annual (and longer term) insolation variation. The strong seasonal variation in the tropical easterlies produces a fluctuating equatorial system (12, 13). In boreal summer at 10°W, easterly wind strength, the speed of the SEC, divergence, and primary productivity are all at maxima, whereas sea-surface temperature (SST) is low, and the nutricline and thermocline lie within the upper euphotic zone (13, 14). In boreal winter at 10°W, the easterly winds weaken and divergence, SEC speed, and primary productivity are all at minima. The nutricline and thermocline lie deep in the euphotic zone and SST is high. Thus the equatorial TBL has two quite different seasonal aspects.

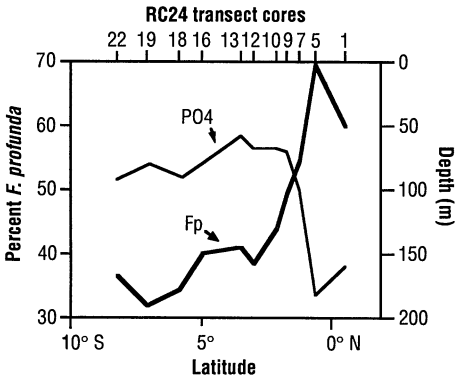

Fig. 2. Plot of percent *F. profunda* (Fp) in a north-south transect of surface sediment samples. The transect extends from 13°39′W (core RC24-1) to 10°01′W (core RC24-22); all transect cores are from water depths shallower than 4000 m. The transect crosses the modern mean axes of flow of both the SEC and EU. The boundary between these two currents occurs between cores RC24-7 and RC24-9, where there is a marked change in both *F. profunda* and the depth of the nutricline, defined here by the depth of the 1.0 μmol liter^{-1} PO_4 value. Phosphate data are from (11).

This annual cycle is an analog for orbitally forced changes (on paleoceanographic time scales) in the tropical easterlies and African monsoon. The stronger the Hadley circulation, the more intense the zonal velocity of the tropical easterlies, Ekman drift, and equatorial divergence. Several global climate models have simulated the atmosphere of 18,000 years ago, the last glacial maximum (15); all these models indicate that the zonality of the tropical easterlies was as strong or stronger than today, when perihelion is aligned with boreal winter. At 9000 years ago, a time when perihelion was aligned with boreal summer, the COHMAP models (16) showed that the meridional component was stronger while the zonal component was weaker relative to both today and the last glacial maximum.

The dynamics of the TBL during the late Pleistocene have been documented by variations in foraminiferal assemblages and estimated SST (17). For the equatorial diver-

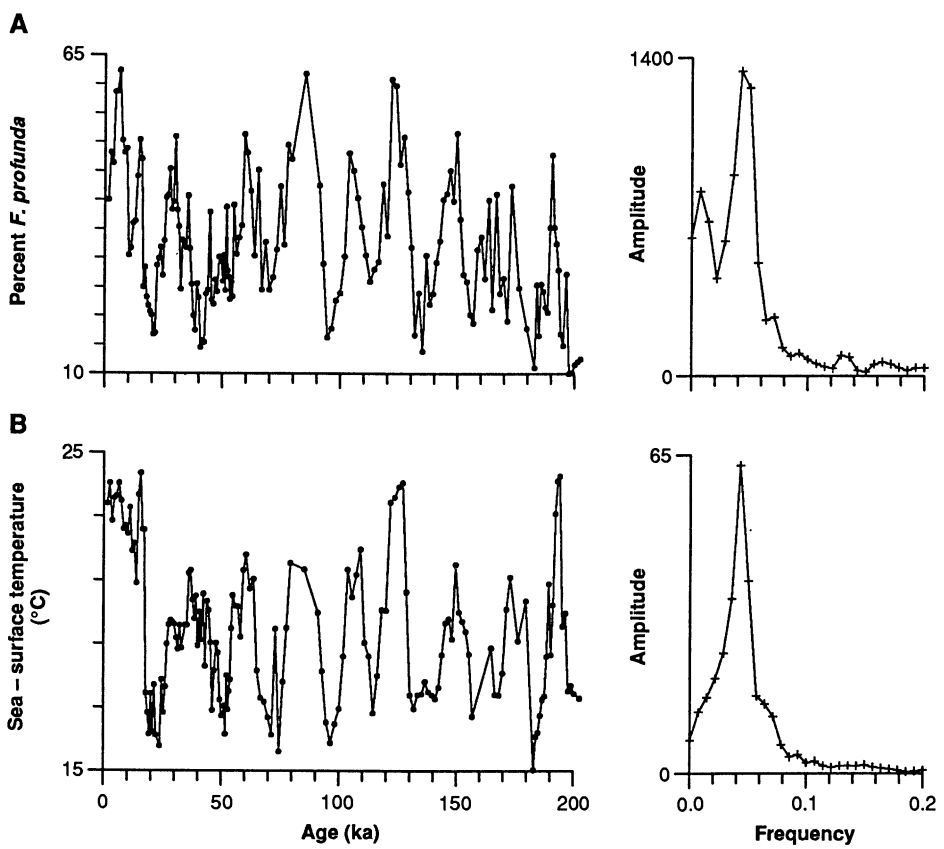

Fig. 3. Time series and spectral signatures from core RC24-7, sited beneath the region of maximum divergence in the equatorial Atlantic. Time series (left) of (**A**) percent *F. profunda*, a monitor of nutricline depth, and (**B**) estimated sea-surface temperature (cold season) based on planktonic foraminifer transfer function AOF20 (21). Data are from the same sediment samples. There is consistency between the occurrence of *F. profunda* minima and sea-surface temperature minima for the last 200,000 years. Variance spectra (right) are dominated by spectral peaks centered on frequency 0.043, equivalent to the 23,000-year periodicity of precession (20); ka, thousand years ago.

gence region of the Atlantic, these signals are dominated by the precessional component (23,000-year period) of orbitally forced variations in insolation. This response is the result of insolation-forced variations in the strength of the tropical easterlies; maximum divergence (minimum SST) occurs when perihelion is aligned with boreal winter (strongest zonality of the tropical easterlies), and vice versa.

To evaluate the relation between nutricline depth and climate forcing, we obtained counts of *F. profunda* at ~1000-year intervals in core RC24-7 (1°20.5′S, 11°53.3′W; 3899 m water depth) for the last 200,000 years. This core is located in the region of maximum divergence. The stratigraphy, foraminiferal response, and estimated SST of this core have been established (*18*) but the chronology has been revised (*19*). Time series of the percentage of *F. profunda* and foraminifer-derived SST (cold season) show a consistent relation: a high percentage of *F. profunda* (deep nutricline) is associated with warm estimated temperatures (minimum divergence), and a low percentage of *F. profunda* (shallow nutricline) is associated with cool estimated temperatures (maximum divergence) (Fig. 3). The cross-correlation coefficient of 0.63 is significant ($P < 0.01$). The signals of the percentage of *F. profunda* and SST, based on the phytoplankton and the zooplankton, respectively, are mutually independent. The constrained amplitudes of these signals suggest that the ocean-climate system is a stationary oscillator at the equator; thus our model is applicable.

Variance spectra of the percentage of *F. profunda* and SST signals for the last 200,000 years are dominated by periodicities centered on the 23,000-year precessional band (Fig. 3). These spectra peaks contain 52 and 53% of the variance of *F. profunda* and SST, respectively. Cross-spectral analysis shows that within the 23,000-year band the signals are coherent ($\kappa = 0.90$) and have a slightly negative phase ($\phi = -25°$), that is, the *F. profunda* signal lags SST by 1500 years, equivalent to 1.5 sampling intervals (*20*). The only visible difference between the two signals is that the *F. profunda* signal contains a secondary spectral peak centered on 100,000 years. Therefore, this 200,000-year record suggests that the dynamic TBL annual cycle is an analog for orbitally forced variations in nutricline depth at precessional periodicities.

The relation between *F. profunda* and the foraminifera in core RC24-7 supports this analogy. The tropical foraminiferal assemblage (abundant when the nutricline is deep and divergence is low) is dominated by *Globigerinoides ruber* (*21*), whose optimum habitat is warm waters of the upper euphotic zone (*22*). The transitional forminiferal assemblage (favored by increased divergence) is dominated by *Globorotalia inflata*, whose optimum habitat is cool waters of the mid to upper euphotic zone. The 23,000-year cycle of *F. profunda* is coherent and in phase with the tropical foraminiferal assemblage, and coherent and out of phase with the transitional foraminiferal assemblage (Table 1).

Table 1. Cross-spectral estimates of coherency and phase, within the 23,000-year band, between *F. profunda* and foraminiferal assemblages in equatorial Atlantic core RC24-7 (*20*). A positive phase angle means variations in *F. profunda* lead variations in the assemblage; a negative phase means the opposite. Phase estimates include their 95% confidence intervals.

Assemblage	Coherency	Phase
Tropical	0.91	−5 ± 24
Transitional	0.83	153 ± 29

Table 2. Comparison of times of occurrence of June perihelion (*23*) with maxima in the abundances of *F. profunda*, and of December perihelion with minima in the abundances of *F. profunda*, in equatorial Atlantic core RC24-7.

Perihelion in June (ka)	*F. profunda* maxima (ka)	Perihelion in Dec. (ka)	*F. profunda* minima (ka)
11	6.4	21	21.0
32	29.9	45	42.3
60	59.3	70	69.8
82	85.1	93	94.6
104	103.6	115	112.6
126	123.4	138	135.0
149	149.5	162	156.8
175	173.0	186	183.0

This unglamorous algae further amazes. In RC24-7, the coldest SST and lowest abundances of *F. profunda* occur when perihelion is aligned with December, boreal winter (Fig. 3 and Table 2). The obverse relation also occurs. McIntyre *et al.* (*17*) showed that when perihelion is centered on boreal summer, equatorial divergence is minimal because the North African monsoon is strong and the zonal component of the tropical easterlies is weak. This relation is corroborated by the near perfect correlation between times of maxima in the percentage of *F. profunda* and perihelion in June, boreal summer (Table 2).

An important objective in paleoceanographic research is the delineation of the TBL heat content, to permit exposition of the oceanic mechanism of heat advection in the TBL. Because the nutricline is linked with the thermocline in tropical waters, paleoceanographic reconstruction of the geometry of the heat reservoir of the tropical-subtropical TBL is possible. In the Neogene, *F. profunda* should provide spatial and temporal estimates of the TBL reservoir volume and heat content, the latter in conjunction with independent biotal temperature estimators.

REFERENCES AND NOTES

1. P. Muller and D. Henderson, Eds., *Dynamics of the Oceanic Surface Mixed Layer* (Spec. Publ., Hawaii Institute of Geophysics, Honolulu, HI, 1987).
2. H. Okada and S. Honjo, *Deep Sea Res.* **20**, 355 (1973).
3. H. Okada and A. McIntyre, *Mar. Biol.* **54**, 319 (1979); *Micropaleontology* **23**, 1 (1977).
4. E. L. Venrick, *Ecol. Monogr.* **52**, 129 (1982).
5. E. L. Crow, F. A. Davis, M. W. Maxfield, *Statistics Manual* (Dover, New York, 1960). From a statistical modeling viewpoint, a number of suitable measures of variation could have been used: the percent of *F. profunda*, the ratio of *F. profunda* to other coccolithophorids, or the log of the ratio of *F. profunda* to other coccolithophorids. As these measures are related by one-to-one transformations, we have elected to use the percent of *F. profunda*.
6. B. Voituriez and A. Herbland, *Deep Sea Res.* **26A**, 77 (1979); A. Herbland, A. Le Bouteiller, P. Raimbault, *ibid.* **32**, 819 (1985).
7. P. L. Richardson and D. Walsh, *J. Geophys. Res.* **91**, 10537 (1986).
8. R. H. Weisberg and T. Y. Yang, *ibid.* **92**, 3709 (1987).
9. C. Henin, P. Hisard, B. Piton, *Observations Hydrologiques dans l'Ocean Atlantique Equatorial (juillet 1982–aout 1984), FOCAL Vol. 1* (Editions de l'Orstom, Paris, 1986).
10. Our usage of the 1.0 μmol of liter^{-1} PO_4 depth-level as the nutricline depth is based on geochemical evidence (B. Molfino and A. McIntyre, unpublished data) from a series of 24 hydrocasts taken within ±3° of latitude along the equator, from 4°W to 20°W, during the South Atlantic Ventilation Experiment (SAVE) and the R. D. Conrad Cruise 24 Leg 3; these data show that the mean position of the 1.0 μmol liter^{-1} PO_4 level is associated with the deeper part of the nutricline.
11. A. G. Kolesnikov, Ed., *Equalant I & II, Oceanographic Atlas* (Unesco Press, Paris-Leningrad, 1976), vol. 2.
12. G. Reverdin, *Deep Sea Res.* **32**, 363 (1985); S. G. H. Philander, *Dyn. Atmos. Oceans* **3**, 191 (1979).
13. J. Servain and D. M. Legler, *J. Geophys. Res.* **91**, 14181 (1986).
14. E. J. Katz and S. L. Garzoli, *Geophys. Res. Lett.* **11**, 737 (1984).
15. J. E. Kutzbach and P. J. Guetter, *J. Atmos. Sci.* **43**, 1726 (1986); S. Manabe and A. J. Broccoli, *J. Geophys. Res.* **90**, 2167 (1985).
16. COHMAP Members, *Science* **241**, 1043 (1988).
17. A. McIntyre *et al.*, *Paloceanography* **4**, 19 (1989).
18. K. Karlin, W. F. Ruddiman, A. McIntyre, *Proc. Ocean Drill. Prog. Sci. Results* **108**, 187 (1989).
19. Revised chronology for core RC24-7 listed as depth and age: 0 cm, 1.5 ka; 33 cm, 7.95 ka; 73 cm, 15.27 ka; 90 cm, 17.8 ka; 115 cm, 21.4 ka; 260 cm, 43.88 ka; 300 cm, 50.21 ka; 345 cm, 54.84 ka; 370 cm, 60.44 ka; 430 cm, 79.25 ka; 440 cm, 90.95 ka; 495 cm, 110.79 ka; 535 cm, 125.19 ka; 565 cm, 135 ka; 620 cm, 151 ka; 640 cm, 156.82 ka; 690 cm, 173 ka; 705 cm, 183 ka; 765 cm, 194 ka; and 780 cm, 197.7 ka.
20. In the spectral and cross-spectral analyses we used equally spaced sampling intervals of 1000 years, 200 sample points, and 70 lags; the bandwidth was 0.019 cycle per 1000 years. The 95% test statistic for nonzero coherency is 0.81. The 95% confidence interval for the reported phase angle is ±18°. We used the standard statistical procedures of G. M. Jenkins and D. G. Watts [*Spectral Analysis and Its Applications* (Holden-Day, San Francisco, 1968)].
21. B. Molfino, N. Kipp, J. Morley, *Quat. Res.* **17**, 279 (1982); SPECMAP archive 1 (Data Support Section, National Center for Atmospheric Research, Boulder, CO, 1989).

22. W. B. Curry, R. C. Thunell, S. Honjo, *Earth Planet. Sci. Lett.* **64**, 33 (1983); R. G. Fairbanks, M. Sverdlove, R. Free, P. H. Wiebe, A. W. H. Be, *Nature* **298**, 841 (1982); W. G. Deuser, E. H. Ross, C. Hemleben, M. Spindler, *Palaeogeogr. Palaeoclimatol. Palaeoecol.* **33**, 103 (1981).
23. A. Berger, *J. Atmos. Sci.* **35**, 2362 (1978).

24. We thank W. F. Ruddiman and C. Sancetta for their critical reviews. This research was supported by NSF grants OCE89-11841 and OCE85-16133. Lamont-Doherty Geological Observatory Contribution No. 4628.

27 March 1990; accepted 4 June 1990

Sequence-Specific DNA Binding by a Short Peptide Dimer

ROBERT V. TALANIAN, C. JAMES MCKNIGHT, PETER S. KIM

A recently described class of DNA binding proteins is characterized by the "bZIP" motif, which consists of a basic region that contacts DNA and an adjacent "leucine zipper" that mediates protein dimerization. A peptide model for the basic region of the yeast transcriptional activator GCN4 has been developed in which the leucine zipper has been replaced by a disulfide bond. The 34-residue peptide dimer, but not the reduced monomer, binds DNA with nanomolar affinity at 4°C. DNA binding is sequence-specific as judged by deoxyribonuclease I footprinting. Circular dichroism spectroscopy suggests that the peptide adopts a helical structure when bound to DNA. These results demonstrate directly that the GCN4 basic region is sufficient for sequence-specific DNA binding and suggest that a major function of the GCN4 leucine zipper is simply to mediate protein dimerization. Our approach provides a strategy for the design of short sequence-specific DNA binding peptides.

THE TRANSCRIPTIONAL ACTIVATOR GCN4 (*1*), which is responsible for the general control of amino acid biosynthesis in yeast (*2*), binds DNA through a structural motif common to several proteins (*3*), including the nuclear oncogene products Fos and Jun. This "bZIP" (*4*) motif consists of a region with several basic residues that probably contacts DNA directly and an adjacent region of about 30 residues containing a heptad repeat of leucines, the "leucine zipper" (*5*), that mediates dimerization. Such bZIP dimers bind DNA sites that are approximately diad-symmetric (*3*).

Structural studies of a synthetic peptide corresponding to the leucine zipper region of GCN4 indicate that the peptide dimerizes as a parallel coiled coil (*6, 7*). The leucine zipper regions are necessary for dimerization of GCN4 (*8–10*) and other bZIP proteins (*11, 12*) and for heterodimer formation by the Fos and Jun proteins (*10, 13–15*). Moreover, synthetic leucine zipper peptides are sufficient for specific homodimer (*6*) and heterodimer (*16*) formation.

The basic region of bZIP proteins is important for DNA binding. Several bZIP proteins with mutations in the basic region fail to bind DNA sequence-specifically although they can dimerize (*12, 13, 17*). Alignment of sequences from different bZIP proteins shows that conserved residues in the basic region and the leucine zipper are separated by an invariant number of residues (*4, 18*). This separation appears crucial since insertion or deletion of a few amino acid residues at the boundary between the two regions can eliminate specific DNA binding activity (*14, 19, 20*). Nevertheless, the two regions appear capable of functioning autonomously, since chimeric bZIP domains (combining the basic region of one protein with the leucine zipper of another) often retain specific DNA binding activity (*10, 20, 21*).

We asked whether the basic region alone, dimerized with a disulfide in place of the leucine zipper, retains sequence-specific DNA binding activity. A peptide (GCN4-brl), corresponding to residues 222 to 252 of GCN4 (*22*), was synthesized (*23*) with a Gly-Gly-Cys linker (*6*) added at the carboxyl terminus (Fig. 1). The glycines were included to provide a flexible linker in the disulfide-bonded dimer, referred to as GCN4-brl^{ss}. The peptide was made as the carboxyl-terminal amide to avoid introduction of additional charge. A second peptide (GCN4-bZIP1), corresponding to the entire bZIP region of GCN4 (residues 222 to 281), was also synthesized (Fig. 1). This 60-residue peptide is capable of dimerization and sequence-specific DNA binding (*8*).

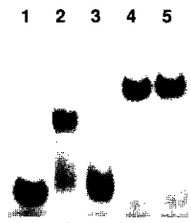

Fig. 2. Gel mobility shift assays (*24*) indicate that DNA binding by GCN4-brl^{ss}, but not GCN4-bZIP1, is sensitive to DTT. Lane 1, no peptide; lane 2, GCN4-brl^{ss}; lane 3, GCN4-brl^{ss} with 10 mM DTT; lane 4, GCN4-bZIP1; and lane 5, GCN4-bZIP1 with 10 mM DTT.

Gel mobility shift assays (*24*) indicate (Fig. 2) that both GCN4-brl^{ss} and GCN4-bZIP1 bind a 20-bp oligonucleotide, GRE20 (*24*), which contains the GCN4 recognition element (GRE) 5′-ATGACTCAT-3′ (*25*). As measured by titration of the gel shift, GCN4-brl^{ss} binds GRE20 with a dissociation constant of ~10 nM at 4°C. Reduction of the disulfide bond in GCN4-brl^{ss} by addition of 10 mM dithiothreitol (DTT) decreases substantially the amount of mobility-shifted DNA, whereas DNA binding by GCN4-bZIP1 is unaffected by this treatment (Fig. 2).

The DNA binding specificities of GCN4-brl^{ss} and GCN4-bZIP1 were tested by using deoxyribonuclease (DNase) I footprinting (*26*). At 4°C both peptides show sequence-specific protection of the GRE site from DNase I digestion (Fig. 3). However, when DNase I digestion was carried out at 24°C, GCN4-brl^{ss} failed to bind specifically, although GCN4-bZIP1 gave an identical footprint to that obtained at 4°C.

The DNA binding specificity of GCN4-brl^{ss} suggests that the peptide is a valid model for the DNA binding activity of GCN4. The binding activity of the peptide dimer demonstrates directly that the basic region of GCN4 (and presumably other bZIP proteins) contains sufficient information for sequence-specific DNA binding. The successful substitution of the leucine

Fig. 1. Sequences of the peptides studied (*23*). GCN4-bZIP1 consists of the 60 carboxyl-terminal residues of GCN4 (*22*). The leucines in the leucine repeat are underlined. GCN4-brl consists of the basic region residues (boxed) plus the carboxyl-terminal linker Gly-Gly-Cys. Abbreviations for the amino acid residues are: A, Ala; C, Cys; D, Asp; E, Glu; G, Gly; H, His; K, Lys; L, Leu; M, Met; N, Asn; P, Pro; Q, Gln; R, Arg; S, Ser; T, Thr; V, Val; and Y, Tyr.

Whitehead Institute for Biomedical Research, Nine Cambridge Center, Cambridge, MA 02142, and Department of Biology, Massachusetts Institute of Technology, Cambridge, MA 02139.